Magnetoelectric effect in bilayer graphene controlled by valley-isospin density

U. Zülicke and R. Winkler

Phys. Rev. B **90**, 125412 — Published 8 September 2014

DOI: 10.1103/PhysRevB.90.125412

Magnetoelectric effect in bilayer graphene controlled by valley-isospin density

U. Zülicke
School of Chemical and Physical Sciences and MacDiarmid Institute for Advanced Materials and Nanotechnology, Victoria University of Wellington, PO Box 600, Wellington 6140, New Zealand and Kavli Institute for Theoretical Physics, University of California, Santa Barbara, CA 93106, USA

R. Winkler
Department of Physics, Northern Illinois University, DeKalb, Illinois 60115, USA Materials Science Division, Argonne National Laboratory, Argonne, Illinois 60439, USA and Kavli Institute for Theoretical Physics, University of California, Santa Barbara, CA 93106, USA

(Dated: August 25, 2014)

We show that bilayer graphene (BLG) exhibits magneto-electric (ME) effects that are formally similar to those commonly seen in band insulators with broken inversion and time-reversal symmetries. Three unusual features characterize the ME responses exhibited by BLG: (i) unlike most other ME media, BLG is a conductor, (ii) BLG has a non-quantized ME coupling even though its electronic structure *does not* break parity and time-reversal symmetry, and (iii) the magnitude of the ME coupling in BLG is determined by the valley-isospin density, which can be manipulated experimentally. This last property also enables a purely electric measurement of valley-isospin densities. While our theoretical arguments use BLG as an example, they are generally valid for any material with similar symmetries.

PACS numbers: 73.22.Pr, 75.85.+t, 03.50.De, 14.80.Va

I. INTRODUCTION AND OVERVIEW OF RESULTS

Ordinarily when matter is exposed to an electric field $\boldsymbol{\mathcal{E}}$ (a magnetic field $\mathbf{B}$), an electric polarization $\mathbf{P}$ (magnetization $\mathbf{M}$) is generated.[1] The magneto-electric (ME) effect[2–4] refers to phenomena where these common relations between applied field and resulting response are crossed; i.e., when an applied electric field produces a finite magnetization and a magnetic field results in an electric polarization of the medium. The constitutive relations between the microscopic fields $\boldsymbol{\mathcal{E}}$, $\mathbf{B}$ and the macroscopic (induced) fields $\mathbf{D}$, $\mathbf{H}$ are then of the general form

$$\mathbf{D} \equiv \epsilon_0 \boldsymbol{\mathcal{E}} + \mathbf{P} = \epsilon_0 \underline{\epsilon} \cdot \boldsymbol{\mathcal{E}} + \underline{\alpha} \cdot \mathbf{B} \quad , \tag{1a}$$

$$\mu_0 \mathbf{H} \equiv \mathbf{B} - \mu_0 \mathbf{M} = \underline{\mu}^{-1} \cdot \mathbf{B} - \mu_0 \underline{\alpha} \cdot \boldsymbol{\mathcal{E}} \quad . \tag{1b}$$

Here $\underline{\epsilon}$, $\underline{\mu}$, and $\underline{\alpha}$ are tensors describing the dielectric, magnetic, and ME response, respectively. The ME tensor is usefully written as[5–7]

$$\underline{\alpha} = \frac{\theta}{2\pi} \frac{e^2}{h} \mathbb{1} + \tilde{\underline{\alpha}} \quad , \tag{2}$$

where $\tilde{\underline{\alpha}}$ is traceless (and, in general, the sum of a symmetric and an antisymmetric part), e denotes the elementary charge, and h is the Planck constant.

Materials exhibiting ME coupling are currently attracting significant interest,[3–9] due to their unconventional basic properties and also because the additional versatility that comes from connecting electric and magnetic phenomena in new ways may become the basis for useful device applications.[4] Due to the different symmetry properties of electric and magnetic fields, ME coupling generally appears in materials in which time-reversal and inversion symmetries are broken.[3,4] Recently it was realized[6] that topological insulators show a *quantized* ME response ($\theta \equiv \pi$, $\tilde{\underline{\alpha}} \equiv 0$). The analogies between the electrodynamic phenomena in topological insulators[6,10,11] and those arising in the context of axion field theory[12] have opened up an intriguing link between condensed-matter and elementary-particle physics.[13]

Here we consider the electromagnetic properties of bilayer graphene (BLG), which is an atomically thin conductor with unusual electronic structure.[14–16] One of the interesting features of charge carriers in BLG is that, in addition to their ordinary (intrinsic) spin, electrons in BLG carry an orbital pseudo-spin-1/2 degree of freedom that is rigidly locked with their linear crystal momentum. Furthermore, states near the Fermi energy exist in two valleys labelled $\mathbf{K}$ and $\mathbf{K'}$ that are conveniently represented by a valley-isospin degree of freedom. Several mechanisms have been proposed to separately address states from the two valleys in BLG[17–23] as part of the recent drive to establish a valleytronics paradigm.[24–26]

Our theoretical study reveals the existence of an unusual ME coupling in BLG that is of the form

$$\theta = 2\pi \frac{n_{\rm v}}{\bar{n}} \quad , \tag{3a}$$

$$\tilde{\underline{\alpha}} = \frac{e^2}{h} \frac{n_{\rm v}}{\bar{n}} \, \eta \begin{pmatrix} 1 & 0 & 0 \\ 0 & 1 & 0 \\ 0 & 0 & -2 \end{pmatrix} \quad , \tag{3b}$$

where $n_{\rm v}$ is the valley-isospin density (i.e., the difference of sheet densities for electrons from the two valleys). Having a finite valley-isospin density corresponds to a non-equilibrium many-particle state that has broken parity and time-reversal symmetry, which enables

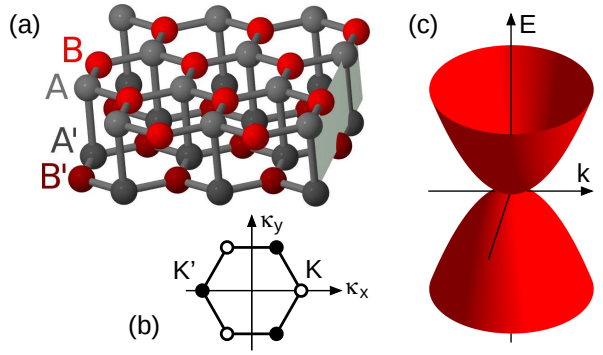

FIG. 1. Basic structural and electronic properties of bilayer graphene. (a) Honeycomb structure of a bilayer stack of graphene. Atoms in sublattice A (B) are marked in grey (red). A yz plane is marked in light grey. (b) Brillouin zone and its two inequivalent corner points $\mathbf{K}$ and $\mathbf{K}'$. The remaining corners are related with $\mathbf{K}$ or $\mathbf{K}'$ by reciprocal lattice vectors. (c) Dispersion $E(\mathbf{k})$ near the $\mathbf{K}$ point. We have $\mathbf{k} \equiv \boldsymbol{\kappa} - \mathbf{K}$.

the ME effect in a system whose band structure has not broken these symmetries.[27] Values for the BLG-specific parameters $\bar{n}$ and η are given below. The dependence on $n_{\rm v}$ establishes an intrinsic link between ME effects and valleytronics in BLG, creating the possibility for electronic control of the generic ramifications of ME coupling[6,12,13,28,29] that is not available in other magnetoelectrics. It is also remarkable in the case of BLG that $\underline{\tilde{\alpha}}$ is finite and θ non-quantized even though time reversal and parity are proper symmetries of this material's bulk electronic structure. As shown by a recent symmetry analysis,[30] the possibility for unconventional couplings between electronic degrees of freedom and electromagnetic fields in BLG arises due to an unusual interplay of time-reversal and spatial symmetries.

Using the well-understood electronic structure of BLG as a specific example, our work establishes a more general paradigm of novel ME phenomena. Indeed, our symmetry-based approach is valid beyond BLG for any materials with similar symmetries. It may guide future research to identify, or even design, materials exhibiting these symmetries that will then also display the ME effects discussed here.

II. MAGNETO-ELECTRIC COUPLING IN BLG

BLG consists of two layers of graphene stacked as shown in Fig. 1(a). Near the $\mathbf{K}$ point in the Brillouin zone [cf. Fig. 1(b)], the low-energy band structure is described by an effective Hamiltonian[14–16]

$$\mathcal{H}^{\mathbf{K}}(\mathbf{k}) = \frac{\hbar^2}{2m_0}\left[-u\left(k_+^2\,\sigma_+ + k_-^2\,\sigma_-\right) + w\,k^2\sigma_0\right] - \hbar v\left(k_-\,\sigma_+ + k_+\,\sigma_-\right)\ , \quad (4)$$

where $\hbar \equiv h/(2\pi)$, $\mathbf{k} \equiv (k_x, k_y)$ is the electrons' wave vector measured from $\mathbf{K}$, the Pauli matrices $\sigma_{x,y,z}$ are associated with the sublattice (or, equivalently, the layer-index) pseudospin degree of freedom, σ_0 is the 2×2 unit matrix, $\sigma_\pm = (\sigma_x \pm i\sigma_y)/2$, and $k_\pm = k_x \pm i k_y$. Numerical values for the effective-mass parameters u, w and the speed v are well known.[14–16] Very close to the $\mathbf{K}$ point, the energy dispersion resulting from Eq. (4) mimics that of massless Dirac electrons, as is the case in single-layer graphene. However, as $u \gg w$, the dominant behavior of electrons in BLG is captured by the quadratic dispersion shown in Fig. 1(c). To obtain the corresponding effective Hamiltonian for electrons in the $\mathbf{K'} = -\mathbf{K}$ valley, we use the relation[31] $\mathcal{H}^{\mathbf{K'}}(\mathbf{k}) = \mathcal{H}^{\mathbf{K}}(R_y^{-1}\mathbf{k})$, where R_y denotes a mirror reflection at the yz plane [see Fig. 1(a)].

The band structure of BLG turns out to be strongly affected by electric and magnetic fields.[14,30,32–39] Combining the electronic degrees of freedom from the two valleys and using a straightforward notation in terms of valley-isospin Pauli matrices τ_0 and τ_z, the effective Hamiltonian becomes $\mathcal{H} = \mathcal{H}_{\rm orb} + \mathcal{H}_{\rm pss} + \mathcal{H}_{\rm ME}$, with

$$\mathcal{H}_{\rm orb} = \sum_{\tau=\pm 1} \frac{\tau_0 + \tau\,\tau_z}{2}\,\mathcal{H}^{\tau\mathbf{K}}(\mathbf{k} + e\mathbf{A}) - e\,\Phi\,\tau_0\ , \quad (5a)$$

$$\mathcal{H}_{\rm pss} = \left(\frac{g_{\rm e}}{2}\,\frac{\mathcal{E}_z}{c}\,\tau_0 - \frac{g_{\rm m}}{2}\,B_z\,\tau_z\right)\mu_{\rm B}\,\sigma_z\quad , \quad (5b)$$

$$\mathcal{H}_{\rm ME} = \left(\xi_\parallel\,\boldsymbol{\mathcal{E}}_\parallel\cdot\mathbf{B}_\parallel + \xi_z\,\mathcal{E}_z B_z\right)e\,\tau_z\quad . \quad (5c)$$

Here $\boldsymbol{\mathcal{E}}_\parallel = (\mathcal{E}_x, \mathcal{E}_y)$ and $\mathbf{B}_\parallel = (B_x, B_y)$, and c is the speed of light in vacuum. The part $\mathcal{H}_{\rm orb}$ contains the coupling of planar electron motion in the BLG sheet to the electromagnetic scalar and vector potentials $\Phi(\mathbf{r})$ and $\mathbf{A}(\mathbf{r})$, respectively, which satisfy $\boldsymbol{\nabla}\Phi + \partial_t\mathbf{A} = -\boldsymbol{\mathcal{E}}_\parallel$ and $\boldsymbol{\nabla}\times\mathbf{A} = B_z\,\hat{\mathbf{z}}$. The effect of external fields on the pseudospin degree of freedom is captured, in lowest order, by $\mathcal{H}_{\rm pss}$, which accounts for the pseudo-spin Zeeman splitting[39] and electric-field-induced bandgap.[14,32–36] In the following, we focus on the ramifications of $\mathcal{H}_{\rm ME}$.

The term $\propto \mathcal{E}_z B_z$ has been discussed previously[37–39] in the context of valley-contrasting magnetic moments. The existence of the complementary coupling of in-plane electric and magnetic field components $\propto \boldsymbol{\mathcal{E}}_\parallel\cdot\mathbf{B}_\parallel$ was recently established by an invariant expansion for the BLG band structure,[30,40] which also revealed the origin of such unconventional terms. Firstly, as in single-layer graphene,[31,41] the two valleys are linked by time-reversal and spatial symmetries in a *combined* way,[40] which results in an unusual constraint on the Hamiltonian describing the intravalley dynamics. From a symmetry perspective, this is the origin for the emergence of massless-Dirac-fermion-like charge carriers in graphitic materials.[31,41] This constraint is likewise satisfied by the terms appearing in $\mathcal{H}_{\rm ME}$. Secondly, and unlike single-layer graphene, the $\mathbf{K}$ point in BLG is characterized by a point group (D_3) that does not distinguish between polar and axial vectors as it only contains rotations as symmetry elements. As a result, components of the electric and magnetic fields are not distinguishable by symmetry and can therefore couple in normally forbidden combinations to electronic degrees of freedom and to each other.[30]

III. LAGRANGIAN FOR ELECTROMAGNETIC FIELDS IN BLG

The terms appearing in $\mathcal{H}_{\rm ME}$ of Eq. (5c) are reminiscent of the $\boldsymbol{\mathcal{E}}\cdot\mathbf{B}$ contribution to the axion Lagrangian.[6,12] They also have a valley dependence. Assuming independent dynamics for electrons from the two valleys, we can define the total sheet density $n_{\rm s}=n^{\mathbf{K}}+n^{\mathbf{K}'}$ and particle-current density $\mathbf{j}_{\rm s}=\mathbf{j}^{\mathbf{K}}+\mathbf{j}^{\mathbf{K}'}$ for electrons from the two valleys as well as the differences $n_{\rm v}=n^{\mathbf{K}}-n^{\mathbf{K}'}$ and $\mathbf{j}_{\rm v}=\mathbf{j}^{\mathbf{K}}-\mathbf{j}^{\mathbf{K}'}$ as relevant variables.[42] They satisfy the continuity equations

$$\partial_t\, n_{\rm s/v}+\boldsymbol{\nabla}\cdot\mathbf{j}_{\rm s/v}=0 \quad . \tag{6}$$

Application of the usual formalism[43] yields the electromagnetic part of the BLG Lagrangian density as

$$\mathcal{L}_{\rm elm}=\mathcal{L}_{\rm Maxwell}+\mathcal{L}_{\rm min}+\mathcal{L}_{\rm ME} \quad . \tag{7a}$$

Here

$$\mathcal{L}_{\rm Maxwell}=\frac{\epsilon_0}{2}\,\boldsymbol{\mathcal{E}}\cdot\underline{\epsilon}\cdot\boldsymbol{\mathcal{E}}-\frac{1}{2\mu_0}\,\mathbf{B}\cdot\underline{\mu}^{-1}\cdot\mathbf{B} \tag{7b}$$

is the familiar Lagrangian for 3D Maxwell electrodynamics in an ordinary medium with, in general, spatially varying dielectric and magnetic tensors $\underline{\epsilon}$ and $\underline{\mu}$, and

$$\mathcal{L}_{\rm min}=-e\left(\mathbf{j}_{\rm s}\cdot\mathbf{A}-n_{\rm s}\,\Phi\right)\delta(z) \tag{7c}$$

is the minimal coupling of the electromagnetic vector and scalar potentials to the electric charge and current densities for electrons in BLG. The part

$$\mathcal{L}_{\rm ME}=-e\,n_{\rm v}\left(\xi_{\parallel}\,\boldsymbol{\mathcal{E}}_{\parallel}\cdot\mathbf{B}_{\parallel}+\xi_z\,\mathcal{E}_z\,B_z\right)\delta(z) \tag{7d}$$

contains the axion-like ME coupling arising from the unconventional contribution (5c) to the BLG Hamiltonian. The fact that the valley-isospin density $n_{\rm v}$ couples to the field combinations in Eq. (7d) is reasonable as $n_{\rm v}$ is odd under both time-reversal and parity transformations. The terms shown in Eq. (7d) are therefore allowed by the symmetry operations applicable to the Lagrangian for the electromagnetic field.

The existence of $\mathcal{L}_{\rm ME}$ leads to modifications of the inhomogeneous Maxwell's equations[12] (i.e., Gauss's and Ampère's laws), resulting in constitutive relations of the form given in Eq. (1) with Eq. (2). Straightforward calculation yields θ and $\tilde{\alpha}$ as given in Eqs. (3), with

$$\bar{n}=\frac{e}{h}\,\frac{3\,d_{\rm eff}}{\xi_z+2\xi_{\parallel}} \quad , \qquad \eta=\frac{\xi_{\parallel}-\xi_z}{\xi_z+2\xi_{\parallel}} \quad . \tag{8}$$

Here $d_{\rm eff}$ denotes the effective electronic width of BLG in the perpendicular (z) direction.

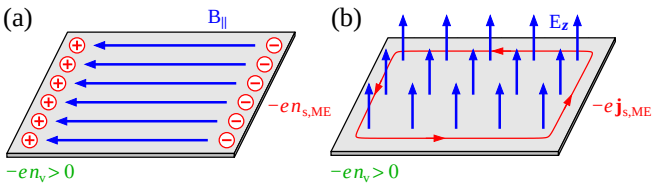

FIG. 2. Illustration of magneto-electric effects in BLG. If the valley-isospin density $n_{\rm v}$ is finite, application of an in-plane magnetic (perpendicular electric) field as shown in panel (a) [(b)] induces charges (currents) at the sample boundary.

IV. MAGNETO-ELECTRIC RESPONSE IN BLG

The modified constitutive relations (1) imply the existence of extra contributions to the total sheet density $n_{\rm s}$ and current $\mathbf{j}_{\rm s}$.[44] In terms of the parameters governing ME responses in BLG, these can be written as

$$n_{\rm s,ME}=-\boldsymbol{\nabla}\cdot\left[n_{\rm v}\left(\xi_{\parallel}\,\mathbf{B}_{\parallel}+\xi_z\,B_z\,\hat{\mathbf{z}}\right)\right], \tag{9a}$$

$$\mathbf{j}_{\rm s,ME}=\boldsymbol{\nabla}\times\left[n_{\rm v}\left(\xi_{\parallel}\,\boldsymbol{\mathcal{E}}_{\parallel}+\xi_z\,\mathcal{E}_z\hat{\mathbf{z}}\right)\right]+\partial_t\left[n_{\rm v}\left(\xi_{\parallel}\,\mathbf{B}_{\parallel}+\xi_z\,B_z\,\hat{\mathbf{z}}\right)\right]. \tag{9b}$$

Obviously, these are nonzero only in case of spatial or temporal variations of the quantities appearing in square brackets in Eqs. (9). For example, the BLG material parameters $\xi_{\parallel}$ and ξ_z are nonzero within BLG but they vanish outside the sample. Thus both their change at the sample boundary as well as any spatial variations of $n_{\rm v}$, $\boldsymbol{\mathcal{E}}$ or $\mathbf{B}$ result in an induced charge density and/or current. We then have

$$n_{\rm s,ME}=-\left[\boldsymbol{\nabla}_{\parallel}\left(n_{\rm v}\,\xi_{\parallel}\right)\right]\cdot\mathbf{B}_{\parallel}-n_{\rm v}\,\xi_{\parallel}\,\boldsymbol{\nabla}\cdot\mathbf{B}_{\parallel}-n_{\rm v}\,\xi_z\,\partial_z B_z. \tag{10}$$

Using the homogeneous Maxwell equation $\boldsymbol{\nabla}\cdot\mathbf{B}=0$, the magnetic-field-induced charge density is found to be

$$n_{\rm s,ME}=-\mathbf{B}_{\parallel}\cdot\boldsymbol{\nabla}\left(n_{\rm v}\,\xi_{\parallel}\right)-n_{\rm v}\left(\xi_{\parallel}-\xi_z\right)\boldsymbol{\nabla}_{\parallel}\cdot\mathbf{B}_{\parallel} \quad . \tag{11}$$

Similarly, inserting the homogeneous Maxwell equation $\boldsymbol{\nabla}\times\boldsymbol{\mathcal{E}}=-\partial_t\mathbf{B}$ into Eq. (9b) yields[45]

$$\mathbf{j}_{\rm s,ME}=\left[\mathcal{E}_z\boldsymbol{\nabla}\left(n_{\rm v}\,\xi_z\right)+n_{\rm v}\left(\xi_z-\xi_{\parallel}\right)\boldsymbol{\nabla}\mathcal{E}_z\right]\times\hat{\mathbf{z}}+\mathbf{B}_{\parallel}\,\partial_t\left(n_{\rm v}\,\xi_{\parallel}\right). \tag{12}$$

Equations (1), (11) and (12) summarize the ME effects in BLG. Charge *densities* are induced by in-plane magnetic fields where $n_{\rm v}$ varies spatially, especially at the BLG sheet's boundaries in the xy plane; and a perpendicular electric field generates in-plane *currents* flowing perpendicular to the spatial gradient of $n_{\rm v}$, especially at the system's boundaries in the xy plane. See Fig. 2 for an illustration. Furthermore, in the likely case[46] that $\xi_{\parallel}\neq\xi_z$, currents (charge densities) are induced in the *bulk* of BLG by spatial inhomogeneity of the perpendicular electric (in-plane magnetic) field component(s) wherever $n_{\rm v}$ is finite, and bulk currents are generated by an *in-plane* magnetic field when $n_{\rm v}\,\xi_{\parallel}$ is time-dependent.

Formally, the ME response of BLG turns out to be analogous to that of a uniaxial ME medium such as Cr_2O_3.[5,29] In particular, the features arising from spatial inhomogeneity of the quantities $n_{\rm v}\,\xi_\parallel$ and $n_{\rm v}\,\xi_z$ are similar to those associated with axion electrodynamics in 3D.[6,12] Given that BLG and ordinary magnetoelectrics belong to very different materials classes (Cr_2O_3 is an antiferromagnetic insulator), this phenomenological similarity is quite surprising. The crucial difference between the two cases is illustrated by the ME parameters. Whereas θ and $\underline{\tilde{\alpha}}$ are fixed in typical ME materials, their values depend on the valley-isospin density $n_{\rm v}$ in BLG.

Generation of a finite $n_{\rm v}$ is possible by various means, including valley-filter contacts,[18–24] optical excitation,[17,47] or using the ME coupling as a source for valley polarization[18,38,39] (cf. discussion below). In the experimentally accessible situation where inter-valley scattering in the relevant part of the sample is weak, the resulting non-equilibrium state with $n_{\rm v} \neq 0$ will be long-lived and enables the observation of ME effects even non-locally (i.e., away from the region where $n_{\rm v}$ is created).

V. MAGNITUDE AND APPLICATION OF MAGNETO-ELECTRIC RESPONSES

The Slonczewski-Weiss-McClure (SWM) model[48] applied to BLG yields in terms of the SWM tight-binding parameters (see also Refs. 38 and 39)

$$\xi_z = \frac{\gamma_0^2}{\gamma_1^2}\,\frac{3\,g_{\rm e}}{8}\,\frac{e}{\hbar}\,\frac{\hbar a^2}{m_0 c} \quad . \tag{13}$$

Recent experiments[36] demonstrated that a vertical electric field of ~ 1 V/nm generates a bandgap of ~ 0.1 eV in BLG, implying $g_{\rm e} \approx 500$ consistent with first-principles calculations.[49] Using the values $\gamma_0 = 3.0$ eV, $\gamma_1 = 0.32$ eV, and $a = 0.245$ nm, we find $\xi_z \approx 6\times 10^{-4}$ nm/T. Assuming furthermore $\xi_\parallel \approx \xi_z$ and $d_{\rm eff} = 0.1$ nm,[49] the parameter $\bar{n} \approx 4\times 10^{12}$ cm^{-2} is obtained from Eq. (8). Thus valley-isospin densities $n_{\rm v} \gtrsim 10^{10}\,{\rm cm}^{-2}$ are expected to generate observable ME effects.

To estimate the magnitude of boundary charges and currents arising from ME coupling in BLG, we use Eqs. (11) and (12) to find

$$n_{\rm s,ME} = -B_\parallel^{(\perp)}\,\frac{d(n_{\rm v}\,\xi_\parallel)}{dr_\perp} \quad , \tag{14a}$$

$$j_{\rm s,ME} = \mathcal{E}_z\,\frac{d(n_{\rm v}\,\xi_z)}{dr_\perp} \quad , \tag{14b}$$

$$I_{\rm ME} \equiv -e\int dr_\perp\;\; j_{\rm s,ME} = -e\,\mathcal{E}_z\,\xi_z\,n_{\rm v} \quad . \tag{14c}$$

Here $r_\perp$ is the in-plane coordinate perpendicular to a chosen boundary of the BLG sample, $B_\parallel^{(\perp)}$ denotes the in-plane magnetic-field component in that perpendicular direction, and $I_{\rm ME}$ is the total charge current flowing parallel to the boundary. Denoting by l the length scale over which the quantity $n_{\rm v}\,\xi_\parallel$ changes at the BLG-sample boundary and assuming $\xi_\parallel \approx \xi_z \sim 6\times 10^{-4}\,{\rm nm/T}$, we find

$$n_{\rm s,ME} \sim B_\parallel^{(\perp)}\,\frac{\xi_\parallel}{l}\,n_{\rm v} \sim 6\times 10^{-4}\;\frac{B_\parallel^{(\perp)}[{\rm T}]}{l[{\rm nm}]}\;n_{\rm v}\,, \tag{15a}$$

$$I_{\rm ME} \sim 10\,{\rm nA}\;\;\mathcal{E}_z\left[\frac{\rm V}{\rm nm}\right]\;\;n_{\rm v}\left[10^{10}\,{\rm cm}^{-2}\right]\,. \tag{15b}$$

According to Eq. (15a), magnetic-field-induced boundary charges are very small for realistic field magnitudes and valley-isospin densities. In contrast, the boundary currents that can be created via the ME effect are definitely measurable, according to Eq. (15b). Detection of these boundary currents can thus be used as a direct measurement of a finite valley-isospin density.

VI. MAGNETO-ELECTRIC COUPLING AS A SOURCE OF VALLEY-ISOSPIN DENSITY

As shown above, charges (currents) are induced in the presence of a finite valley-isospin density and a magnetic (electric) field by virtue of the ME coupling. In short, a finite $n_{\rm v}$ plus *one type* of field give rise to a total-charge or current response. These effects embody the emergent electromagnetism in BLG. Conversely, the ME coupling affects the electronic structure of a BLG sample in the *simultaneous presence of parallel electric and magnetic fields*, introducing a uniform energy shift for electron levels that is opposite in the two valleys. It is clear that such an effect must introduce a valley-isospin density, as electrons redistribute from one valley to the other in order to keep a constant Fermi energy throughout the system. Initially, only the term $\propto \mathcal{E}_z\,B_z$ was known, and a careful treatment of it (taking account of the orbital effects of B_z, i.e., Landau quantization) indeed found that a valley-isospin density is generated.[18,38,39]

The term $\propto \xi_\parallel\,\boldsymbol{\mathcal{E}}_\parallel\cdot\mathbf{B}_\parallel$ imposes the same type of energy shift and thus also induces a valley-isospin density, which we can estimate to be[50]

$$n_{\rm v} = \frac{2}{\pi}\,\frac{e\,m_0}{\hbar^2}\,\frac{\xi_\parallel}{u}\,\mathcal{E}_\parallel\,B_\parallel \sim \mathcal{E}_\parallel\left[\frac{V}{\rm mm}\right]\;B_\parallel[T]\times 10^{12}\,{\rm cm}^{-2}. \tag{16}$$

Here we assumed $\xi_\parallel \sim \xi_z \approx 6\times 10^{-4}$ nm/T to obtain the numerical value given on the r.h.s. of Eq. (16). In contrast to the situation involving field components perpendicular to the sheet, the magnetic field $\mathbf{B}_\parallel$ has no orbital consequences. However, $\boldsymbol{\mathcal{E}}_\parallel$ couples electrostatically to the *total* charge density and gets screened from the interior of a conducting BLG sample. Thus, it will at most induce a finite $n_{\rm v}$ at the boundary over a distance of the screening length.

VII. CONCLUSIONS

Fundamental symmetry considerations reveal the presence of a valley-contrasting magneto-electric coupling (5c) for electrons in bilayer graphene.[18,30,38,39] As a result, the Lagrangian governing the co-operative dynamics of electrons and electromagnetic fields has a contribution where the valley-isospin density couples to the parity- and time-reversal-odd terms $\propto \boldsymbol{\mathcal{E}}_{\parallel} \cdot \mathbf{B}_{\parallel}$ and $\mathcal{E}_z B_z$ [cf. Eq. (7d)]. The resulting non-quantized magneto-electric response of bilayer graphene mirrors that of conventional uniaxial magneto-electric media, which is unusual because the latter are typically insulating materials whose electronic degrees of freedom exhibit broken parity and time-reversal symmetry.[27] The unexpected behavior of electrons in graphene bilayers arises because constraints due to invariance under time reversal and parity involve the two valleys, rendering the dynamics of electrons within individual valleys qualitatively different from that of ordinary charge carriers. In particular, the intra-valley dynamics in bilayer graphene cannot distinguish between polar and axial vectors[30] and, as a result, supports the magneto-electric coupling discussed here. As the validity of our symmetry-based approach is not restricted to bilayer graphene, other materials with similar properties are likely to exist or become available in the future.

Linking valleytronics with magneto-electric effects establishes new pathways for each of these fields. For example, the dependence of the magneto-electric effects in bilayer graphene on the valley-isospin density allows one to detect such charge imbalances between the valleys, e.g., via the boundary currents generated by a perpendicular electric field. Also, the unusual electrodynamic properties exhibited by magnetoelectrics[28,29] become tunable in bilayer graphene by controlling its valley-isospin densities and currents.

ACKNOWLEDGMENTS

This research was supported by the NSF under Grant No. DMR-1310199 and, at KITP, by Grant No. PHY11-25915. Work at Argonne was supported by DOE BES under Contract No. DE-AC02-06CH11357. Useful discussions with J. J. Heremans, A. H. MacDonald, and I. Martin are gratefully acknowledged.

[1] J. D. Jackson, *Classical Electrodynamics*, 3rd ed. (Wiley, Hoboken, NJ, 1999).
[2] T. H. O'Dell, *The Electrodynamics of Magneto-electric Media* (North-Holland, Amsterdam, 1970).
[3] M. Fiebig, J. Phys. D **38**, R123 (2005).
[4] R. Ramesh and N. A. Spaldin, Nat. Mater. **6**, 21 (2007).
[5] F. W. Hehl, Y. N. Obukhov, J.-P. Rivera, and H. Schmid, Phys. Lett. A **372**, 1141 (2008).
[6] X.-L. Qi, T. L. Hughes, and S.-C. Zhang, Phys. Rev. B **78**, 195424 (2008).
[7] A. M. Essin, A. M. Turner, J. E. Moore, and D. Vanderbilt, Phys. Rev. B **81**, 205104 (2010).
[8] R. Li, J. Wang, X.-L. Qi, and S.-C. Zhang, Nat. Phys. **6**, 284 (2010).
[9] H. Ooguri and M. Oshikawa, Phys. Rev. Lett. **108**, 161803 (2012).
[10] J. E. Moore, Nature (London) **464**, 194 (2010).
[11] X.-L. Qi and S.-C. Zhang, Rev. Mod. Phys. **83**, 1057 (2011).
[12] F. Wilczek, Phys. Rev. Lett. **58**, 1799 (1987).
[13] M. Franz, Physics **1**, 36 (2008).
[14] E. McCann and V. I. Fal'ko, Phys. Rev. Lett. **96**, 086805 (2006).
[15] A. H. Castro Neto, F. Guinea, N. M. R. Peres, K. S. Novoselov, and A. K. Geim, Rev. Mod. Phys. **81**, 109 (2009).
[16] E. McCann and M. Koshino, Rep. Prog. Phys. **76**, 056503 (2013).
[17] W. Yao, D. Xiao, and Q. Niu, Phys. Rev. B **77**, 235406 (2008).
[18] D. Xiao, W. Yao, and Q. Niu, Phys. Rev. Lett. **99**, 236809 (2007).
[19] I. Martin, Y. M. Blanter, and A. F. Morpurgo, Phys. Rev. Lett. **100**, 036804 (2008).
[20] D. S. L. Abergel and T. Chakraborty, Appl. Phys. Lett. **95**, 062107 (2009).
[21] H. Schomerus, Phys. Rev. B **82**, 165409 (2010).
[22] G. Y. Wu, N.-Y. Lue, and Y.-C. Chen, Phys. Rev. B **88**, 125422 (2013).
[23] L. Pratley and U. Zülicke, Appl. Phys. Lett. **104**, 082401 (2014).
[24] A. Rycerz, J. Tworzydło, and C. W. J. Beenakker, Nat. Phys. **3**, 172 (2007).
[25] O. Gunawan, Y. P. Shkolnikov, K. Vakili, T. Gokmen, E. P. De Poortere, and M. Shayegan, Phys. Rev. Lett. **97**, 186404 (2006).
[26] K. Behnia, Nat. Nanotech. **7**, 488 (2012).
[27] The ME effects focused on in this work arise in the presence of a finite $n_{\rm v}$ and either an electric *or* a magnetic field. Here, the non-equilibrium many-particle state with a finite $n_{\rm v}$ effectively breaks parity and time-reversal symmetry, even though these are good symmetries for the BLG band structure. In contrast, these symmetries are broken in the band structure of ordinary ME media. In BLG, in the presence of (static) parallel electric *and* magnetic fields, $n_{\rm v}$ is finite in equilibrium.
[28] D. I. Khomskii, arXiv:1307.2327.
[29] M. Fechner, N. A. Spaldin, and I. E. Dzyaloshinskii, Phys. Rev. B **89**, 184415 (2014).
[30] R. Winkler and U. Zülicke, arXiv:1206.4761.
[31] R. Winkler and U. Zülicke, Phys. Rev. B **82**, 245313 (2010).
[32] E. McCann, Phys. Rev. B **74**, 161403 (2006).
[33] T. Ohta, A. Bostwick, T. Seyller, K. Horn, and E. Rotenberg, Science **313**, 951 (2006).
[34] H. Min, B. Sahu, S. K. Banerjee, and A. H. MacDonald,

Phys. Rev. B **75**, 155115 (2007).
[35] E. V. Castro, K. S. Novoselov, S. V. Morozov, N. M. R. Peres, J. M. B. L. dos Santos, J. Nilsson, F. Guinea, A. K. Geim, and A. H. C. Neto, Phys. Rev. Lett. **99**, 216802 (2007).
[36] Y. Zhang, T.-T. Tang, C. Girit, Z. Hao, M. C. Martin, A. Zettl, M. F. Crommie, Y. R. Shen, and F. Wang, Nature **459**, 820 (2009).
[37] M. Nakamura, E. V. Castro, and B. Dóra, Phys. Rev. Lett. **103**, 266804 (2009).
[38] M. Koshino and T. Ando, Phys. Rev. B **81**, 195431 (2010).
[39] L. M. Zhang, M. M. Fogler, and D. P. Arovas, Phys. Rev. B **84**, 075451 (2011).
[40] G. L. Bir and G. E. Pikus, *Symmetry and Strain-Induced Effects in Semiconductors* (Wiley, New York, 1974).
[41] J. L. Mañes, F. Guinea, and M. A. H. Vozmediano, Phys. Rev. B **75**, 155424 (2007).
[42] The sheet densities and current densities are obtained by integrating the corresponding three-dimensional electronic densities over the z coordinate perpendicular to the BLG plane. Also, in this work, components of the electric and magnetic field represent averages of these quantities over the finite thickness of the BLG sample.
[43] See, e.g., E. Fradkin, *Field Theories of Condensed Matter Physics*, 2nd ed. (Cambridge University Press, Cambridge, UK, 2013). A related calculation for BLG subject to crossed electric and magnetic fields was recently performed by M. Katsnelson, G. Volovik, and M. Zubkov, Ann. Phys. (NY) **331**, 160 (2013).
[44] In the previously encountered situations where the ME medium is an insulator, these are associated with bound charges. In BLG, they correspond to free charges.
[45] In arriving at Eq. (12), the term

$$\boldsymbol{\mathcal{E}}_\parallel \times \boldsymbol{\nabla}\left(n_\mathrm{v}\,\xi_\parallel\right) - \left[B_z\,\partial_t\left(n_\mathrm{v}\,\xi_z\right) + n_\mathrm{v}\left(\xi_z - \xi_\parallel\right)\partial_t B_z\right]\hat{\mathbf{z}}$$

has been omitted for two reasons. Firstly, $\mathbf{j}_\mathrm{s}$ can only have in-plane components. Secondly, and more importantly, the above contribution arises due to an *in-plane electric* or *perpendicular magnetic* field, both of which strongly affect the orbital motion of electrons in the BLG sheet. In contrast, the presence of *perpendicular electric* or *in-plane magnetic* fields will not lead to drastic orbital effects and, therefore, reveal clearly the ME effects discussed here.
[46] The value of $\xi_\parallel$ is currently not known.
[47] K. F. Mak, K. L. McGill, J. Park, and P. L. McEuen, Science **344**, 1489 (2014).
[48] J. W. McClure, Phys. Rev. **108**, 612 (1957).
[49] S. Konschuh, M. Gmitra, D. Kochan, and J. Fabian, Phys. Rev. B **85**, 115423 (2012).
[50] The valley-asymmetric energy shifts $\propto \mathcal{E}_z\,B_z$, $\boldsymbol{\mathcal{E}}_\parallel \cdot \mathbf{B}_\parallel$ are part of the effective low-energy-Hamiltonian description that applies only at energies well below the interlayer coupling energy $\gamma_1 \approx 0.32\,\mathrm{eV}$. Hence there exists an upper bound $n_\mathrm{v} \ll 2m_0\gamma_1/(\pi\hbar^2 u) \approx 8\times 10^{12}\,\mathrm{cm}^{-2}$ to the valley-isospin density that can be generated by this mechanism.